Avicenna Journal of Phytomedicine (AJP)

Original Research Article

Ginsenoside Rb1 suppresses microglial neuroinflammation through an A2A receptor- and Gαs-sensitive mechanism

Yang Zhao[1], Xin Dong[2], Yiting Wang[1], Junbo Cui[2], Runxuan Xin[1], Bayan Yeerlan[1], Wenfeng Zhang[1], Yi Dai[3], Jianmei Huang[2], Minke Tang[1,*]

[1]*Department of Pharmacology, School of Chinese Materia Medica, Beijing University of Chinese Medicine, Beijing 100029, China*
[2]*Department of Analytical Chemistry, School of Chinese Materia Medica, Beijing University of Chinese Medicine, Beijing 100029, China*
[3]*Department of Anatomy and Neuroscience, School of Medicine, Hyogo Medical University, Nishinomiya 663-8501, Japan*

Article history:
Received: Jul 16, 2026
Received in revised form: Aug 04, 2026
Accepted: Aug 15, 2026
Epub ahead of print

**** Corresponding Author:***
tangmk@bucm.edu.cn

Keywords:
Ginsenoside Rb1
Adenosine A2A receptor
Microglia
Neuroinflammation
Lipopolysaccharides
Cytokines

Abstract

Objective: Ginsenoside Rb1, a major saponin component of *Panax ginseng*, exhibits anti-inflammatory and neuroprotective effects, but its receptor-associated mechanism in microglia remains incompletely defined. This study investigated whether Rb1 suppresses microglial neuroinflammation through an adenosine A2A receptor (A2AR)-associated, Gαs-sensitive mechanism.

Materials and Methods: Rb1 concentration in brain tissue after repeated systemic administration was quantified by ultra-high-performance liquid chromatography-high-resolution mass spectrometry. Anti-inflammatory effects were evaluated in a lipopolysaccharide (LPS)-induced mouse neuroinflammation model and in LPS-stimulated BV2 microglial cells. Pharmacological blockade with the Gαs inhibitor NF449 and the A2AR antagonist ZM241385 was used to examine pathway sensitivity. Molecular docking was performed to explore the possible spatial relationship between Rb1 and adenosine-bound A2AR.

Results: Intraperitoneally administered Rb1 reached measurable brain concentrations of 30.88 ± 0.94 ng/mg protein 24 hr after injection. Rb1 reduced LPS-induced brain levels of tumor necrosis factor-α, interleukin-1β, interleukin-6, and interleukin-10. In BV2 cells, Rb1 attenuated LPS-induced cytokine production at non-cytotoxic concentrations, while Rb1 alone did not alter basal cytokine release. The anti-inflammatory effects of Rb1 were reduced by NF449 and ZM241385. Docking suggested that Rb1 may localize within the extracellular vestibule of adenosine-bound A2AR without overlapping with the orthosteric adenosine-binding site.

Conclusion: These findings support an A2AR-associated, Gαs-sensitive anti-inflammatory mechanism for Rb1 in microglia and provide a receptor-level basis for further mechanistic studies.

Please cite this paper as:
Zhao Y, Dong X, Wang Y, Cui J, Xin R, Yeerlan B, Zhang W, Dai Y, Huang J, Tang M. Ginsenoside Rb1 suppresses microglial neuroinflammation through an A2A receptor- and Gαs-sensitive mechanism. Avicenna J Phytomed, 2026

Introduction

Neuroinflammation is a common feature of many neurological disorders and is closely linked to sustained activation of microglia. Activated microglia release inflammatory mediators such as tumor necrosis factor-α, interleukin-1β, and interleukin-6, which can aggravate neuronal injury when produced excessively or persistently (Glass et al. 2010; Jurgens and Johnson 2012; Smith et al. 2012; Heneka et al. 2015; Colonna and Butovsky 2017; Leng and Edison 2021; Beheshtimanesh and Rajaei 2022). Therefore, pharmacological regulation of microglial inflammatory responses remains an important strategy for limiting neuroinflammatory damage.

Ginsenoside Rb1 (Figure1), a major saponin component of *Panax ginseng*, has shown anti-inflammatory and neuroprotective activities in several experimental models including reduction of inflammatory cytokine production and modulation of intracellular inflammatory pathways such as NF-κB-related signaling (Ahmed et al. 2016; Wang et al. 2018; Shaukat et al. 2021; Zhang et al. 2021; Ni et al. 2022; Ji et al. 2024; Liu et al. 2025; Pu et al. 2025). However, these findings mainly describe downstream inflammatory responses, while the upstream receptor-associated mechanisms by which Rb1 regulates glial inflammatory activity remain insufficiently defined (Zhuang et al. 2025). In a previous work, we showed that Rb1 protects astrocytes against oxygen-glucose deprivation/reoxygenation-induced injury through a GPCR-$G_{\alpha s}$-related mechanism (Wang et al. 2024). These observations raised the possibility that a related receptor-associated mechanism may also contribute to the regulation of microglial inflammation by Rb1.

G protein-coupled receptors are key regulators of microglial function. Among them, the adenosine A2A receptor (A2AR) is a major $G_{\alpha s}$-coupled receptor involved in the control of microglial inflammatory responses. Activation of A2AR has been associated with suppression of inflammatory mediator production in microglia and other immune cells (Marala and Mustafa 1998; Harada et al. 2000; Morello et al. 2006; Csóka et al. 2007; Newell et al. 2015; Ansari et al. 2017; Skopál et al. 2022; Cheng et al. 2025). On this basis, we examined whether A2AR contributes to the anti-inflammatory action of Rb1 in microglia.

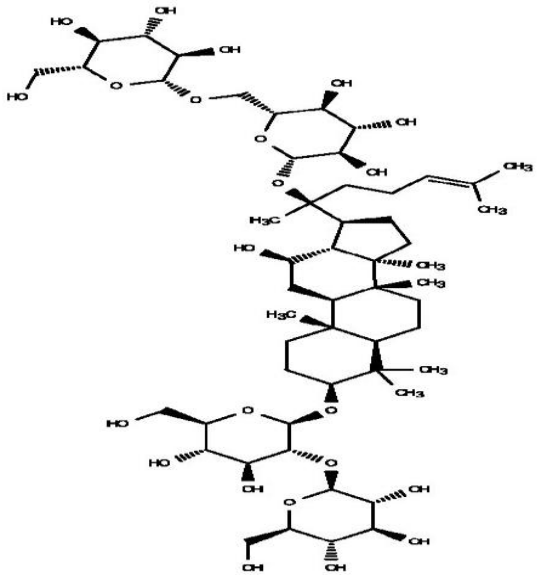

Figure 1. Chemical structure of ginsenoside Rb1

In this study, we first quantified Rb1 concentration in brain tissue after repeated systemic administration using ultra-high-performance liquid chromatography-high-resolution mass spectrometry. We then examined the effects of Rb1 on Lipopolysaccharides (LPS)-induced cytokine production in mouse brain and BV2 microglial cells. Finally, we used pharmacological blockade of Gαs and A2AR, together with molecular docking, to assess whether Rb1 suppresses microglial inflammation through an A2AR-associated, Gαs-sensitive mechanism.

Materials and Methods

Reagents

Ginsenoside Rb1 (purity >98%) was purchased from Chengdu MUST Biotech Co., Ltd. (Chengdu, China).

Lipopolysaccharide (LPS; *Escherichia coli* O55:B5) was obtained from Merck KGaA (Darmstadt, Germany). Cell Counting Kit-8 (CCK-8; C6005) was purchased from NCM Biotech (Suzhou, China). ELISA kits for interleukin-1β (IL-1β) (KT2040-A), interleukin-6 (IL-6) (KT2163-A), tumor necrosis factor-α (TNF-α) (KT2132-A), and interleukin-10 (IL-10) (KT2176-A) were obtained from Kete Biotech (Jiangsu, China). NF449 (HY-112461A) and ZM241385 (HY-19532) were purchased from MedChemExpress (Monmouth Junction, NJ, USA).

Animals and treatments

Male ICR mice aged 8–10 weeks were obtained from SPF (Beijing) Biotech Co., Ltd. (Beijing, China). Mice were acclimatized for one week before experiments and housed under controlled temperature conditions (23 ± 2 °C) with a 12-hr light/dark cycle and free access to standard chow and water. All procedures were approved by the Institutional Animal Care and Use Committee of Beijing University of Chinese Medicine (Approval No. BUCM20251218-002) and were performed in accordance with the approved protocol and national regulations for laboratory animal welfare.

Mice were randomly assigned to three groups: Control (n = 5), LPS (n = 5), and LPS + Rb1 (n = 8). Mice in the LPS + Rb1 group received Rb1 (20 mg/kg, intraperitoneally, dissolved in normal saline (0.9% NaCl)) once daily for seven consecutive days. Mice in the Control and LPS groups received an equivalent volume of normal saline. On day 7, one hour after the final Rb1 or saline administration, mice in the LPS and LPS + Rb1 groups were challenged with a single intraperitoneal injection of LPS (3 mg/kg, prepared in normal saline (0.9% NaCl) with brief sonication before use), whereas control mice received normal saline. Brain tissues were collected 24 hr after LPS injection.

For detection of Rb1 levels in brain tissue, three mice were randomly selected from the LPS + Rb1 group. The remaining five mice in this group were used for cytokine analysis. Brain tissues were homogenized in normal saline and analyzed as described below.

Detection of ginsenoside Rb1 in brain

Rb1 concentration in brain tissue was quantified at 24 hr after LPS challenge, corresponding to the time of tissue collection. Brain tissues were homogenized in normal saline (0.9% NaCl) at a ratio of 1 mL per 100 mg tissue, and an aliquot of each homogenate was reserved for total protein determination using a bicinchoninic acid (BCA) assay. For Rb1 extraction, 500 μL of brain homogenate was mixed with 1.5 mL of ice-cold acetonitrile for protein precipitation. After vortexing and centrifugation at 12,000×g for 10 min at 4° C, the supernatant was evaporated to dryness under a nitrogen stream at 37°C. The residue was reconstituted in 100 μL of mobile phase and centrifuged again at 12,000 × g for 10 min at 4 °C. The resulting supernatant was used for UHPLC-HRMS analysis.

Rb1 was quantified using a matrix-matched external standard method. Calibration curves were prepared by spiking Rb1 reference standard into blank mouse brain homogenate at known concentrations. The instrumental limit of detection and limit of quantification for Rb1 were 62.5 pg and 250 pg, respectively. Rb1 levels were normalized to total protein content. The brain Rb1 values in this study should be regarded as semi-quantitative and primarily serve to support the presence of Rb1 in brain tissue following repeated systemic administration.

UHPLC-HRMS analysis was performed using an ACQUITY UPLC system (Waters, Milford, MA, USA) coupled to a Q Exactive Plus Hybrid Quadrupole-Orbitrap Mass Spectrometer (Thermo Fisher Scientific, Waltham, MA, USA). Chromatographic separation was achieved on a BEH C18 column (2.1 × 100 mm, 1.7 μm) using a gradient of 0.1%

formic acid in water and acetonitrile at a flow rate of 0.25 mL/min. The mobile phase gradient was as follows: 0-2 min, 5% acetonitrile; 2-12 min, 5-85% acetonitrile; 12-14 min, 85% acetonitrile; 14-15 min, 85-5% acetonitrile; and 15-20 min, 5% acetonitrile. The injection volume was 5 μL, and the column temperature was maintained at 35 °C. Ionization was performed using a heated electrospray ionization source (HESI) in negative ion mode. Targeted quantification was conducted using parallel reaction monitoring in negative ion mode. The precursor ion for Rb1 was set at m/z 1153.6012 $[M + HCOO]^-$, with a monitored product ion at m/z 1107.5957 $[M - H]^-$. Data were processed using Xcalibur software.

BV2 cell culture and treatments

BV2 murine microglial cells were cultured in Dulbecco's Modified Eagle Medium (DMEM) containing 10% fetal bovine serum and 1% penicillin/streptomycin in a humidified incubator at 37°C with 5% CO_2.

For cytotoxicity assessment, cells were seeded in 96-well plates at a density of 1×10^4 cells per well. After 24 hr, the medium was replaced with fresh DMEM containing Rb1 at the indicated concentrations. After another 24 hr, cell viability was measured using the CCK-8 assay according to the manufacturer's instructions.

To evaluate the protective effects of Rb1 against LPS-induced injury, BV2 cells were treated with LPS (0.5 μg/mL) in the presence or absence of Rb1 at the indicated concentrations. Rb1 and LPS were freshly prepared and added simultaneously to the culture medium. After 24 hr, cell viability was assessed using the CCK-8 assay.

For receptor-blockade experiments, BV2 cells were pretreated with NF449 or ZM241385 for 60 or 30 min (Teresa Bengoechea-Alonso et al. 2003; Peart and Gross 2006; Lin et al. 2011; Tozzi et al. 2007), respectively, before treatment with Rb1 and LPS. Samples were collected 24 hr later for cytokine measurement.

Enzyme-linked immunosorbent assay (ELISA)

Cytokine levels of TNF-α, IL-1β, IL-6, and IL-10 were measured using ELISA kits according to the manufacturer's instructions. For *in vivo* experiments, brain homogenates were used. For *in vitro* experiments, culture supernatants were collected after treatment. Cytokine levels in brain tissue were normalized to total protein content, whereas cytokine concentrations in culture supernatants are reported as absolute values.

Molecular docking

Molecular docking simulations were performed using the CB-Dock2 server, which combines curvature-based cavity detection with AutoDock Vina for binding pose prediction. The human adenosine A2A receptor structure bound to adenosine (PDB ID: 2YDO) was used as the docking template.

To assess the docking protocol, adenosine was first removed from the crystal structure and re-docked into the receptor. The reproduced binding pose was compared with the crystallographic position of adenosine. The re-docked adenosine pose showed a Vina binding affinity score of −7.1 kcal/mol and an RMSD of 0.68Å from the crystallographic adenosine position, supporting the validity of the docking protocol.

Rb1 was then docked into the adenosine-occupied receptor, with adenosine retained in the orthosteric pocket. The search space was set to include the extracellular vestibule region. The top-ranked Rb1 pose was selected according to the Vina binding affinity score and visual inspection of its location relative to the adenosine-occupied orthosteric site.

PyMOL was used for visualization and figure preparation.

Statistical analysis

Data are presented as mean ± SEM. Group differences were analyzed by one-way ANOVA with Welch's correction. Post hoc comparisons were performed using Dunnett's T3 multiple comparisons test for experiments involving comparison with a single reference group, and Šídák's multiple comparisons test for pre-selected pairwise comparisons among multiple groups. Statistical analyses were performed using GraphPad Prism version 10.6.0 (GraphPad Software, San Diego, CA, USA). A value of $p<0.05$ was considered statistically significant.

Results

Detection of ginsenoside Rb1 in mouse brain after systemic administration

Repeated systemic administration of Rb1 (20 mg/kg, intraperitoneally) resulted in measurable Rb1 concentrations in brain tissue as determined by UHPLC-HRMS. Brain extracts from Rb1-treated mice showed a chromatographic peak at 8.92 min in the extracted ion chromatogram of the m/z 1153.6012→1107.5957 transition, closely matching the retention time of the Rb1 reference standard at 8.88 min, whereas no corresponding peak was detected in blank naïve brain extracts, confirming the absence of endogenous interference (Figure 2A). The identity of Rb1 was further supported by the product-ion (MS/MS) spectrum of the m/z 1153.6012 $[M + HCOO]^-$precursor, which yielded product ions at m/z 1107.5999 $[M-H]^-$, 945.5482, 783.4935, 621.4393, and 459.3855 (Figure 2B).

2A

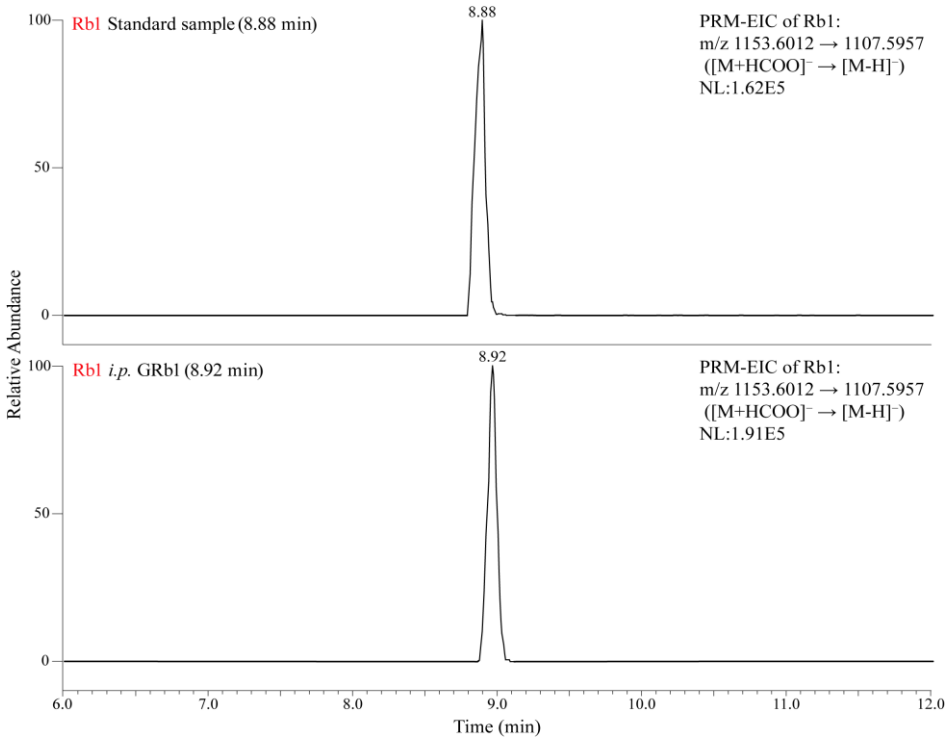

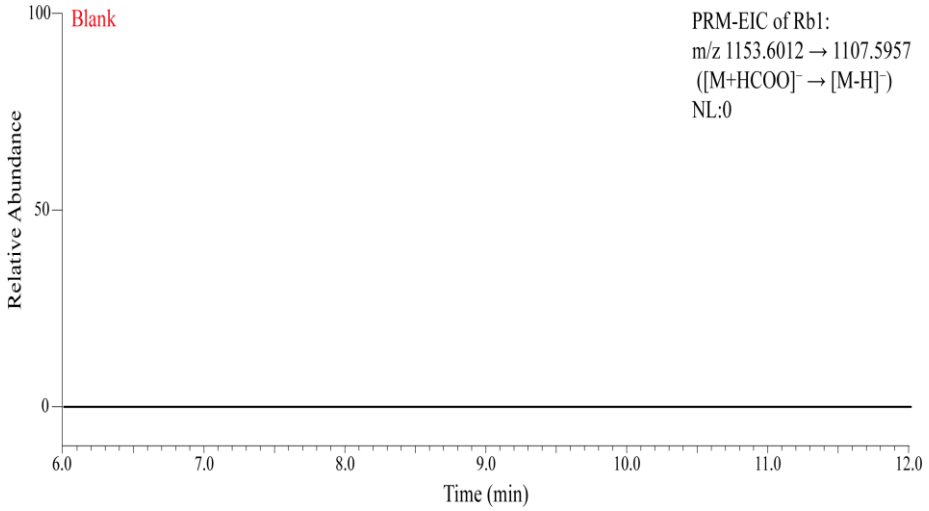

2B

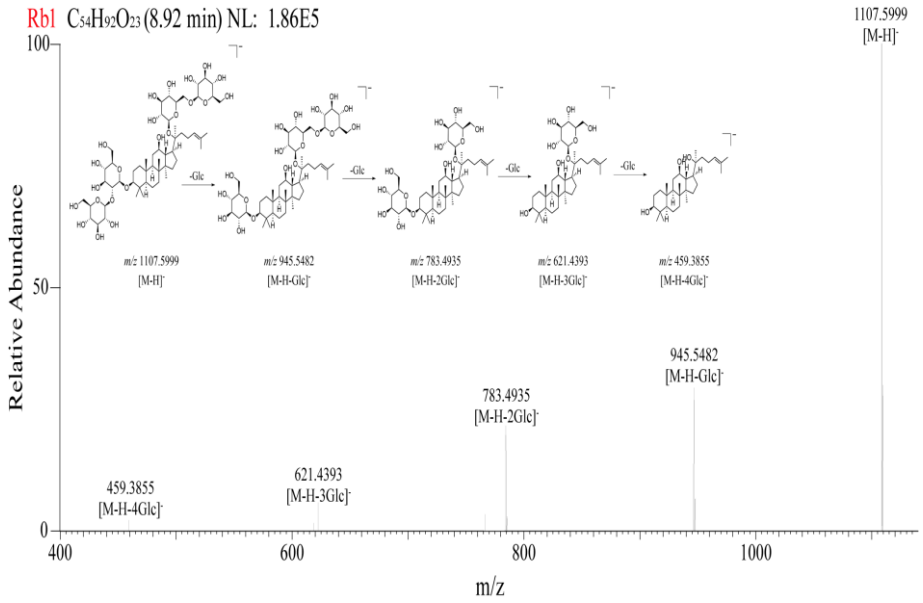

Figure 2. Detection and structural support for ginsenoside Rb1 in mouse brain following systemic administration.(A) Representative extracted ion chromatograms (EICs) acquired by parallel reaction monitoring (PRM) in negative ion mode for the Rb1 reference standard (top), a brain tissue extract from the LPS + Rb1 group (middle), and a blank naïve brain extract processed identically (bottom). The EICs were extracted using the transition m/z 1153.6012 ($[M + HCOO]^-$) → 1107.5957 ($[M - H]^-$) with a mass tolerance of ±5 ppm. Matched peaks were observed at 8.88 min (standard) and 8.92 min (brain extract), whereas no peak was detected at the corresponding retention time in the blank, confirming the absence of endogenous interference. (B) The identity of Rb1 was further supported by the product-ion (MS/MS) spectrum of the m/z 1153.6012 $[M + HCOO]^-$ precursor, showing characteristic fragment ions at m/z 1107.5999, 945.5482, 783.4935, 621.4393, and 459.3855. Rb1 brain concentrations were quantified by UHPLC-HRMS and normalized to total protein content (30.88 ± 0.94 ng/mg protein; n = 3).

Quantification normalized to total protein content showed a mean brain Rb1 level of 30.88 ± 0.94 ng/mg protein in the LPS+Rb1 group (n=3), corresponding to approximately 1,544 ± 47 ng/g brain tissue (estimated using ~50 mg protein per gram tissue, based on homogenization of 100 mg brain in 1 mL saline at ~5 mg/mL protein), measured at 24 hr after LPS challenge.

Rb1 attenuates LPS-induced cytokine production in the brain

To examine whether Rb1 affects neuroinflammatory responses *in vivo*, cytokine levels were measured in brain homogenates after systemic LPS challenge. LPS markedly increased brain levels of TNF-α, IL-1β, IL-6, and IL-10 compared with the control group (Figure 3). Treatment with Rb1 (20 mg/kg) reduced the LPS-induced increases in TNF-α, IL-1β, and IL-6. Rb1 also lowered the LPS-induced elevation of IL-10 (Figure 3), suggesting an overall reduction in the inflammatory response rather than selective suppression of pro-inflammatory cytokines. The attenuation of IL-10 most likely reflects a reduction in the overall LPS-driven inflammatory response, including its compensatory anti-inflammatory arm, consistent with the parallel reductions observed in pro-inflammatory cytokines.

To determine whether microglia may contribute to this effect, we next examined the action of Rb1 in BV2 microglial cells.

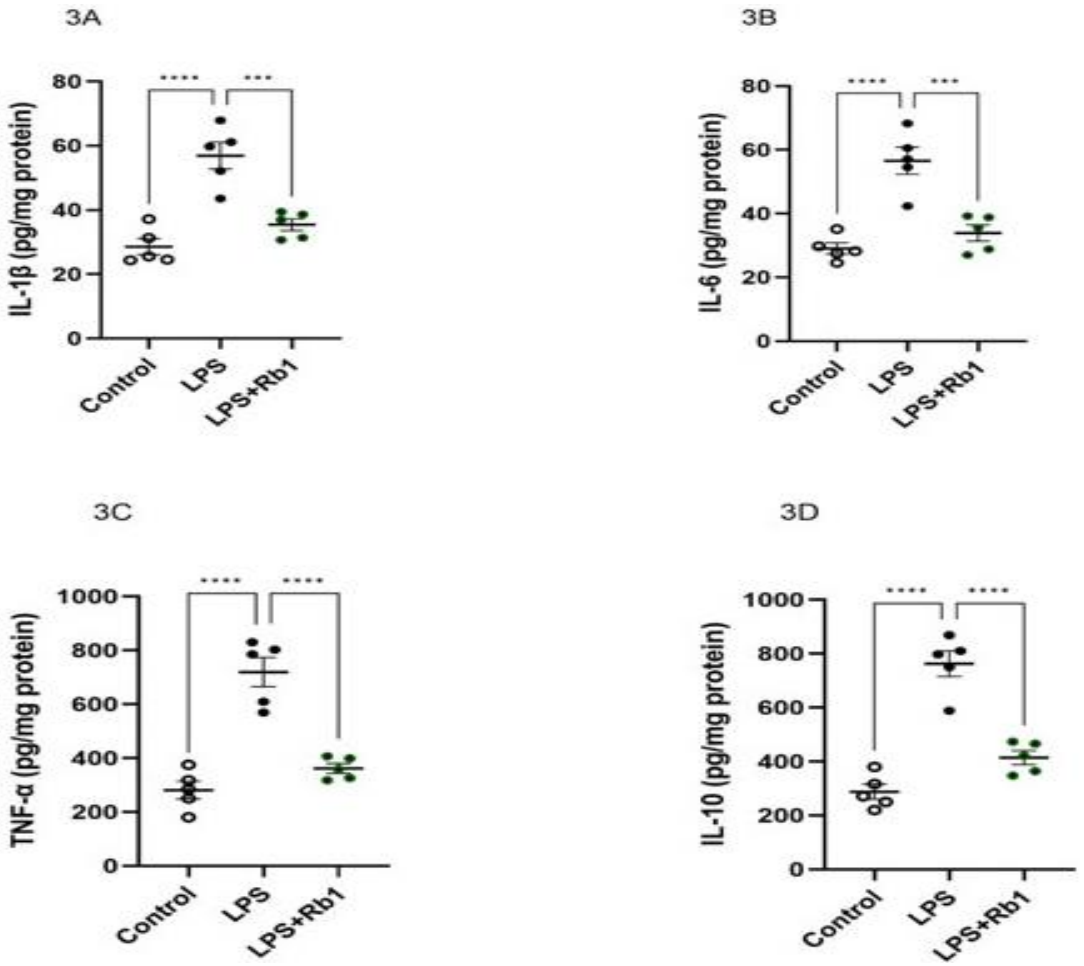

Figure 3. Ginsenoside Rb1 attenuates LPS-induced cytokine production in mouse brain. Levels of IL-1β (A), IL-6 (B), TNF-α (C), and IL-10 (D) were measured by ELISA in brain homogenates from the Control, LPS, and LPS + Rb1 groups. LPS increased cytokine levels compared with the control group. Treatment with Rb1 (20 mg/kg, intraperitoneally) reduced the LPS-induced elevations of IL-1β, IL-6, TNF-α, and IL-10. Data are presented as mean ± SEM (n = 5 mice per group). ***p<0.001; ****p<0.0001.

Rb1 protects BV2 cells against LPS-induced cytotoxicity

We first examined the effects of Rb1 on BV2 cell viability to define a non-toxic concentration range. BV2 cells were treated with Rb1 at concentrations from 0.01 to 100 μM for 24 hr. Rb1 did not significantly affect cell viability at concentrations up to 1 μM, whereas concentrations of 10 μM and above reduced viability (Figure 4A). Therefore, concentrations no higher than 1 μM were used in subsequent experiments.

LPS treatment (0.5 μg/mL) reduced BV2 cell viability to approximately 70% of the control level (Figure 4B). Co-treatment with Rb1 restored cell viability in a concentration-dependent manner, with 1 μM Rb1 increasing viability to nearly 90% of the control level. These results indicate that Rb1 protects BV2 cells against LPS-induced cytotoxicity at non-toxic concentrations. Based on the non-toxic concentration range and the protective response observed in the viability assay, 100 nM Rb1 was selected for subsequent cytokine and receptor-blockade experiments.

We next examined whether 100 nM Rb1 affected inflammatory cytokine production in BV2 cells.

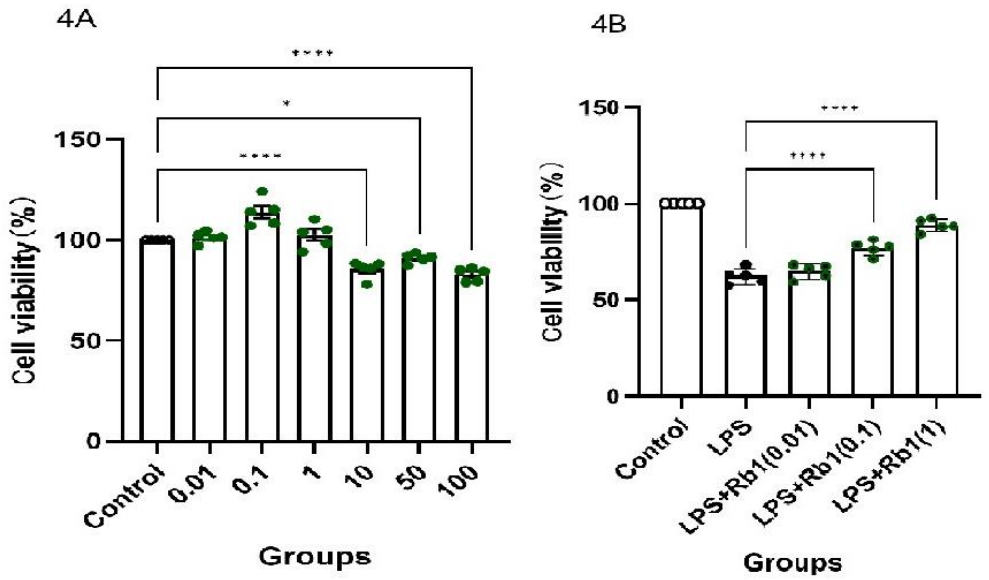

Figure 4. Ginsenoside Rb1 protects BV2 cells against LPS-induced cytotoxicity. (A) Concentration-dependent effects of Rb1 on BV2 cell viability. BV2 cells were treated with Rb1 at concentrations from 0.01 to 100 μM for 24 h, and viability was measured using the CCK-8 assay. Rb1 did not affect cell viability at concentrations up to 1 μM, whereas higher concentrations reduced viability. Numbers on the x-axis indicate Rb1 concentrations in μM. (B) Effects of Rb1 on LPS-induced cytotoxicity. BV2 cells were co-treated with LPS (0.5 μg/mL) and Rb1 (0.01, 0.1, or 1 μM) for 24 hr. Rb1 restored cell viability compared with the LPS group. Data are presented as mean ± SEM (n = 5 independent experiments, each performed in triplicate). *p<0.05; ****p<0.0001.

Rb1 suppresses LPS-induced cytokine production through a $G_{\alpha s}$-sensitive mechanism

To examine whether Gαs signaling contributes to the anti-inflammatory effect of Rb1, BV2 cells were pretreated with the $G_{\alpha s}$ inhibitor NF449 (1 μM). LPS markedly increased the secretion of IL-1β, IL-6, TNF-α, and IL-10 (Figure 5). Treatment with Rb1 (100 nM) reduced the LPS-induced increases in these cytokines. Pretreatment with NF449 attenuated the effect of Rb1, with cytokine levels returning toward those observed in the LPS-treated group. These results indicate that the cytokine-suppressive effect of Rb1 is sensitive to pharmacological inhibition of Gαs.

Rb1 suppresses LPS-induced cytokine production in an A2AR-sensitive manner

To examine whether A2AR contributes to the anti-inflammatory effect of Rb1, BV2 cells were pretreated with the A2AR antagonist ZM241385 (300 nM). LPS markedly increased the secretion of IL-1β, IL-6, TNF-α, and IL-10 (Figure 6). Treatment with Rb1 (100 nM) reduced the LPS-induced increases in these cytokines. Pretreatment with ZM241385 attenuated the effect of Rb1, with cytokine levels returning toward those observed in the LPS-treated group. Rb1 alone did not significantly alter basal cytokine release in unstimulated BV2 cells. These results indicate that the cytokine-suppressive effect of Rb1 is sensitive to pharmacological blockade of A2AR.

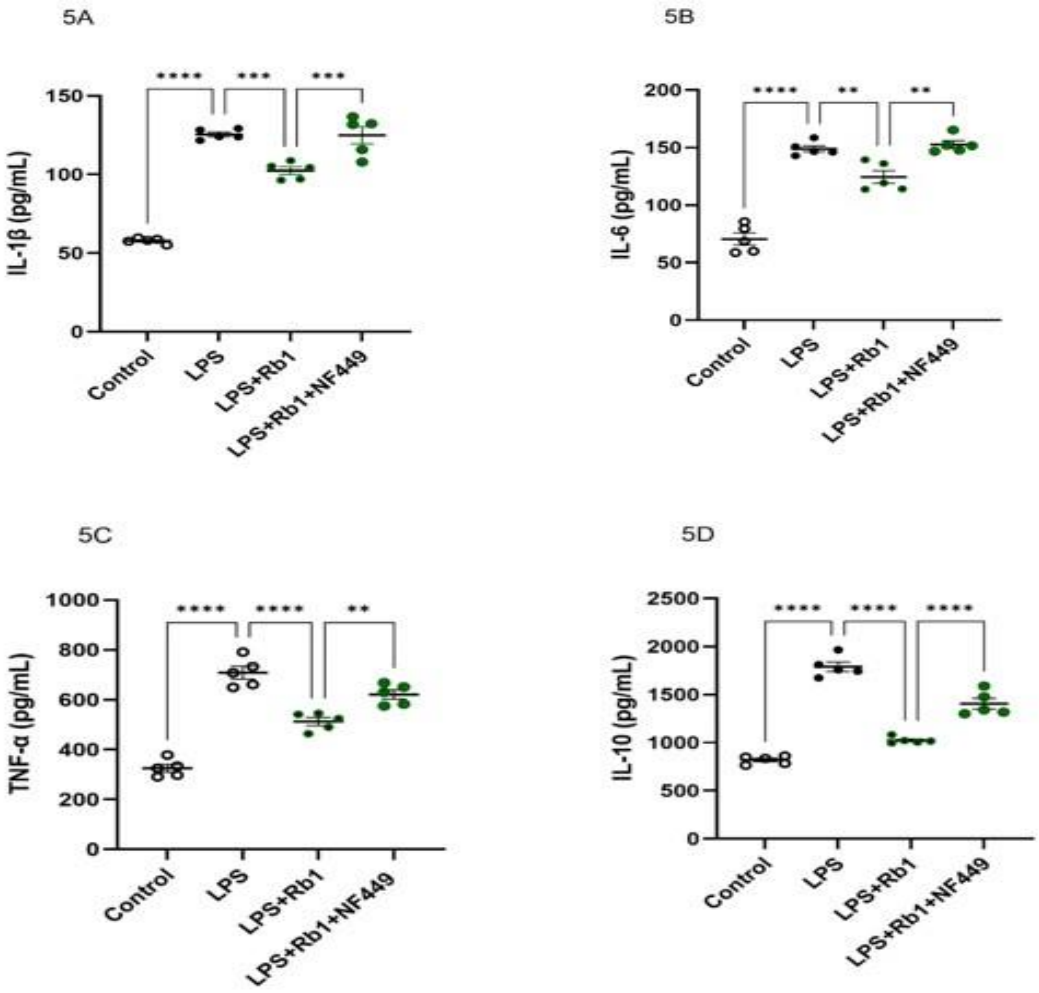

Figure 5. Ginsenoside Rb1 suppresses LPS-induced cytokine production in a $G_{\alpha s}$-sensitive manner. BV2 cells were pretreated with the $G_{\alpha s}$ inhibitor NF449 (1 μM) for 60 min before co-treatment with LPS (0.5 μg/mL) and Rb1 (100 nM) for 24 hr. Cytokine levels of IL-1β (A), IL-6 (B), TNF-α (C), and IL-10 (D) in culture supernatants were quantified by ELISA. Rb1 reduced LPS-induced cytokine production. Pretreatment with NF449 attenuated the effect of Rb1, with cytokine levels returning toward those observed in the LPS-treated group. Data are presented as mean ± SEM (n = 5 independent experiments, each performed in triplicate). **p<0.01; ***p<0.001; ****p<0.0001.

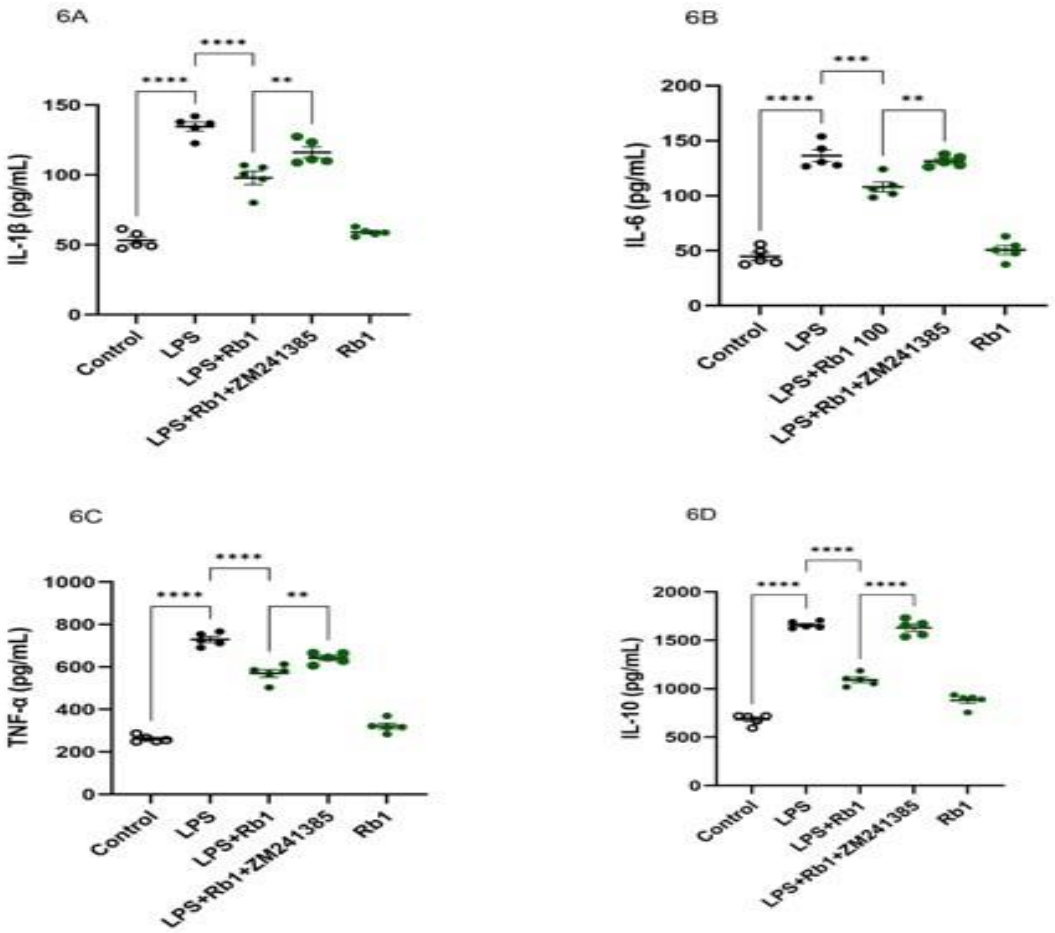

Figure 6. Ginsenoside Rb1 suppresses LPS-induced cytokine production in an A2AR-sensitive manner. BV2 cells were pretreated with the A2AR antagonist ZM241385 (300 nM) for 30 min before co-treatment with LPS (0.5 μg/mL) and Rb1 (100 nM) for 24 hr. Cytokine levels of IL-1β (A), IL-6 (B), TNF-α (C), and IL-10 (D) in culture supernatants were quantified by ELISA. Rb1 reduced LPS-induced cytokine production. Pretreatment with ZM241385 attenuated the effect of Rb1, with cytokine levels returning toward those observed in the LPS-treated group. Rb1 alone did not significantly alter basal cytokine release in unstimulated BV2 cells. Data are presented as mean ± SEM (n = 5 independent experiments, each performed in triplicate). **p<0.01; ***p<0.001; ****p<0.0001.

Molecular docking suggests extracellular vestibule binding of Rb1 in adenosine-occupied A2AR

To explore a possible structural basis for the A2AR-associated effect of Rb1, molecular docking was performed using the adenosine-bound A2AR structure (PDB ID: 2YDO). After validation of the docking protocol by re-docking adenosine into the receptor, Rb1 was docked into the adenosine-occupied receptor.

Rb1 was predicted to localize within the extracellular vestibule, at a site spatially distinct from the adenosine-occupied orthosteric pocket (Figure 7A), with a Vina binding affinity score of −8.2 kcal/mol. The predicted pose involved vestibule-region residues including Asn175, His264, Lys150, and Tyr271 (Figure 7B). Phe168 and Glu169 were located near the boundary between the extracellular vestibule and the adenosine-occupied orthosteric pocket. No obvious steric overlap between Rb1 and adenosine was observed in the docking model.

Together with the pharmacological data, this docking result suggests that the extracellular vestibule of A2AR may contribute to the receptor-associated action of Rb1.

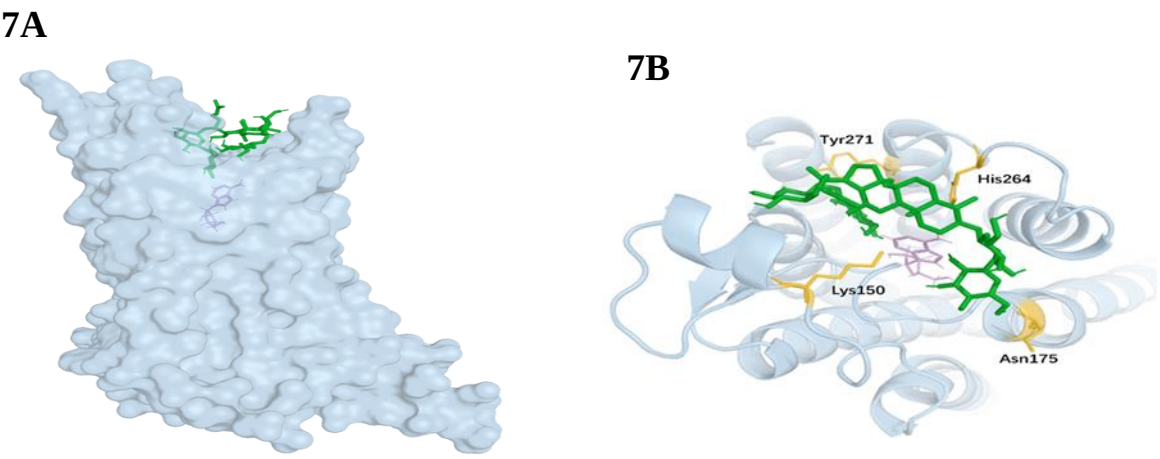

Figure 7. Molecular docking suggests extracellular vestibule localization of Rb1 in adenosine-occupied A2AR. (A) Surface representation of the human adenosine A2A receptor (PDB: 2YDO; pale blue) showing the predicted binding pose of ginsenoside Rb1 within the extracellular vestibule and adenosine in the orthosteric pocket. Rb1 localizes above the orthosteric site without obvious steric overlap with adenosine in the docking model. (B) Close-up cartoon representation of the binding region showing selected vestibule-region residues near the predicted Rb1 pose (Lys150, Asn175, His264, and Tyr271). Rb1 is shown in green, adenosine in muted purple, and selected residues in gold. Adenosine is shown in the orthosteric pocket for spatial reference.

Discussion

In this study, Rb1 reduced LPS-induced inflammatory cytokine production in mouse brain and BV2 microglial cells. UHPLC-HRMS analysis detected Rb1 in brain tissue after systemic administration. In BV2 cells, the cytokine-suppressive effect of Rb1 was attenuated by NF449 and ZM241385, suggesting involvement of a Gαs-sensitive and A2AR-associated mechanism. Molecular docking further suggested that Rb1 may occupy the extracellular vestibule of adenosine-bound A2AR without obvious overlap with the orthosteric adenosine-binding site.

The detection of Rb1 in brain tissue is important because the high molecular weight and polarity of Rb1 have raised questions about its central exposure after systemic administration (Kim 2013; Kim et al. 2023; Wang et al. 2025). In the present study, UHPLC-HRMS analysis showed measurable Rb1 levels in brain homogenates after intraperitoneal treatment. This finding supports the possibility that Rb1 can act within the central nervous system, although the exact route of brain entry and the free concentration available at receptor sites remain to be clarified.

A2AR is a $G_{\alpha s}$-coupled receptor involved in the regulation of inflammatory responses in microglia and other immune cells (Taskén and Aandahl 2004; Hamano et al. 2008; Orr et al. 2009; Rebola et al. 2011; Melani et al. 2014; Cunha 2016). In the present study, ZM241385 attenuated the cytokine-suppressive effect of Rb1, supporting the involvement of an A2AR-associated mechanism. NF449 produced a similar attenuation, indicating that the effect of Rb1 is also sensitive to pharmacological inhibition of $G_{\alpha s}$. These findings are consistent with our previous observation that Rb1 protected astrocytes against oxygen–glucose deprivation/reoxygenation-induced injury through a GPCR–$G_{\alpha s}$-related mechanism. Together, the present results suggest that GPCR–Gαs-related signaling may be a shared component of the glial protective actions of Rb1, while identifying A2AR as a plausible receptor-associated contributor to its anti-inflammatory effect in microglia.

The docking analysis provides structural context for the pharmacological

observations (Christopoulos 2002; May et al. 2007; Jeffrey Conn et al. 2009). Rb1 was predicted to localize mainly within the extracellular vestibule of A2AR, supporting the possibility that this extracellular region may contribute to the receptor-associated action of Rb1.

It should be acknowledged that blockade of $G_{\alpha s}$ and A2AR with more delicate grouping assignment (including Rb1 alone group) during *in vivo* study will further help decipher the mechanisms of Rb1. Direct $G_{\alpha s}$ signaling readouts, including cAMP accumulation, protein kinase A (PKA) activation, and cAMP response element-binding protein (CREB) phosphorylation, will provide more definitive confirmation of the downstream signaling pathway. A full and detailed pharmacokinetic sampling, including plasma, represents an important objective for future investigation as well.

Taken together, this study shows that ginsenoside Rb1 reaches measurable levels in mouse brain after repeated systemic administration and suppresses LPS-induced inflammatory cytokine production *in vivo* and in BV2 microglial cells. Its effect was sensitive to pharmacological blockade of $G_{\alpha s}$ and A2AR, supporting an A2AR-associated, Gαs-sensitive mechanism. Molecular docking further suggests a possible role for the extracellular vestibule of A2AR in this receptor-associated action.

Acknowledgment

This work was supported by the Beijing Science and Technology Program (Grant No. Z251100007125032), National Administration of Traditional Chinese Medicine Program (Grant No.2541STC72909), and National Key Research and Development Program of China (Grant No.2026YFE0201000).

Conflicts of interest

The authors have declared that there is no conflict of interest.

Funding

This work was supported by the Beijing Science and Technology Program (Grant No. Z251100007125032), National Administration of Traditional Chinese Medicine Program (Grant No.2541STC72909), and National Key Research and Development Program of China (Grant No.2026YFE0201000).

Ethical Considerations

The experimental procedures received approval from the Ethics Committee at Beijing University of Chinese Medicine. We took every possible measure to reduce animal suffering and to decrease the study's animal usage.

Code of Ethics

BUCM20251218-002

Authors' Contributions

Yang Zhao and Yiting Wang performed the in vivo experiments and cytokine analyses. Xin Dong and Junbo Cui developed and validated the UHPLC-HRMS analytical method and performed brain concentration quantification. Runxuan Xin, Bayan Yeerlan, and Wenfeng Zhang contributed to in vitro cell culture experiments and data collection. Jianmei Huang supervised the analytical chemistry work. Yi Dai contributed anatomical and neuroscience expertise. Minke Tang conceived and designed the study, supervised all experimental work, interpreted the data, and wrote the manuscript. All authors reviewed and approved the final manuscript.

References

Ahmed T, Raza SH, Maryam A, et al (2016) Ginsenoside Rb1 as a neuroprotective agent: A review. Brain Res Bull 125:30–43. https://doi.org/10.1016/j.brainresbull.2016.04.002

Ansari MA, Nadeem A, Attia SM, et al (2017) Adenosine A2A receptor modulates neuroimmune function through Th17/retinoid-related orphan receptor

gamma t (RORγt) signaling in a BTBR T + Itpr3 tf /J mouse model of autism. Cell Signal 36:14–24. https://doi.org/10.1016/j.cellsig.2017.04.014

Beheshtimanesh Z, Rajaei Z (2022) Neuroprotective effects of sesamol against LPS-induced spatial learning and memory deficits are mediated via anti-inflammatory and antioxidant activities in the rat brain. Avicenna J Phytomedicine. https://doi.org/10.22038/ajp.2022.21403

Cheng C, Cheng W, Wang Y, et al (2025) The Dual Role of A2aR in Neuroinflammation: Modulating Microglial Polarization in White Matter Lesions. eneuro 12:ENEURO.0579-24.2025. https://doi.org/10.1523/ENEURO.0579-24.2025

Christopoulos A (2002) Allosteric binding sites on cell-surface receptors: novel targets for drug discovery. Nat Rev Drug Discov 1:198–210. https://doi.org/10.1038/nrd746

Colonna M, Butovsky O (2017) Microglia Function in the Central Nervous System During Health and Neurodegeneration. Annu Rev Immunol 35:441–468. https://doi.org/10.1146/annurev-immunol-051116-052358

Csóka B, Németh ZH, Virág L, et al (2007) A2A adenosine receptors and C/EBPβ are crucially required for IL-10 production by macrophages exposed to Escherichia coli. Blood 110:2685–2695. https://doi.org/10.1182/blood-2007-01-065870

Cunha RA (2016) How does adenosine control neuronal dysfunction and neurodegeneration? J Neurochem 139:1019–1055. https://doi.org/10.1111/jnc.13724

Glass CK, Saijo K, Winner B, et al (2010) Mechanisms underlying inflammation in neurodegeneration. Cell 139:1218–1241

Hamano R, Takahashi HK, Iwagaki H, et al (2008) Stimulation of adenosine a2a receptor inhibits lps-induced expression of intercellular adhesion molecule 1 and production of tnf-α in human peripheral blood mononuclear cells. Shock 29:154–159. https://doi.org/10.1097/shk.0b013e31812385da

Harada N, Okajima K, Murakami K, et al (2000) Adenosine and selective A(2A) receptor agonists reduce ischemia/reperfusion injury of rat liver mainly by inhibiting leukocyte activation. J Pharmacol Exp Ther 294:1034–1042

Heneka MT, Carson MJ, Khoury JE, et al (2015) Neuroinflammation in Alzheimer's disease. Lancet Neurol 14:388–405. https://doi.org/10.1016/S1474-4422(15)70016-5

Jeffrey Conn P, Christopoulos A, Lindsley CW (2009) Allosteric modulators of GPCRs: a novel approach for the treatment of CNS disorders. Nat Rev Drug Discov 8:41–54. https://doi.org/10.1038/nrd2760

Ji L, Han H, Shan X, et al (2024) Ginsenoside Rb1 ameliorates lipotoxicity-induced myocardial injury in diabetes mellitus by regulating Mfn2. Eur J Pharmacol 974:176609. https://doi.org/10.1016/j.ejphar.2024.176609

Jurgens HA, Johnson RW (2012) Dysregulated neuronal–microglial cross-talk during aging, stress and inflammation. Exp Neurol 233:40–48. https://doi.org/10.1016/j.expneurol.2010.11.014

Kim H-K (2013) Pharmacokinetics of ginsenoside Rb1 and its metabolite compound K after oral administration of Korean Red Ginseng extract. J Ginseng Res 37:451–456. https://doi.org/10.5142/jgr.2013.37.451

Kim S-W, Han B-C, So S-H, et al (2023) Biodistribution and pharmacokinetic evaluation of Korean Red Ginseng components using radioisotopes in a rat model. J Ginseng Res 47:74–80. https://doi.org/10.1016/j.jgr.2022.05.001

Leng F, Edison P (2021) Neuroinflammation and microglial activation in Alzheimer disease: where do we go from here? Nat Rev Neurol 17:157–172. https://doi.org/10.1038/s41582-020-00435-y

Lin AHY, Leung GPH, Leung SWS, et al (2011) Genistein enhances relaxation of the spontaneously hypertensive rat aorta by transactivation of epidermal growth factor receptor following binding to membrane estrogen receptors-α and activation of a G protein-coupled, endothelial nitric oxide synthase-dependent pathway. Pharmacol Res 63:181–189. https://doi.org/10.1016/j.phrs.2010.11.007

Liu R, Zhao X, Zhu Y, et al (2025) Ginsenoside Rb1 attenuates neuroflammation via activating Wnt/β-catenin signaling pathway to exert neuroprotective effect on cerebral ischemic-reperfusion injury. Front Aging Neurosci 17:1555067. https://doi.org/10.3389/fnagi.2025.1555067

Marala RB, Mustafa SJ (1998) Immunological characterization of adenosine A2A receptors in human and porcine cardiovascular tissues. J Pharmacol Exp Ther 286:1051–1057

May LT, Leach K, Sexton PM, Christopoulos A (2007) Allosteric Modulation of G Protein–Coupled Receptors. Annu Rev Pharmacol Toxicol 47:1–51. https://doi.org/10.1146/annurev.pharmtox.47.120505.105159

Melani A, Corti F, Cellai L, et al (2014) Low doses of the selective adenosine A2A receptor agonist CGS21680 are protective in a rat model of transient cerebral ischemia. Brain Res 1551:59–72. https://doi.org/10.1016/j.brainres.2014.01.014

Morello S, Ito K, Yamamura S, et al (2006) IL-1β and TNF-α Regulation of the Adenosine Receptor (A2A) Expression: Differential Requirement for NF-κB Binding to the Proximal Promoter. J Immunol 177:7173–7183. https://doi.org/10.4049/jimmunol.177.10.7173

Newell EA, Exo JL, Verrier JD, et al (2015) 2′,3′-cAMP, 3′-AMP, 2′-AMP and adenosine inhibit TNF-α and CXCL10 production from activated primary murine microglia via A2A receptors. Brain Res 1594:27–35. https://doi.org/10.1016/j.brainres.2014.10.059

Ni X-C, Wang H-F, Cai Y-Y, et al (2022) Ginsenoside Rb1 inhibits astrocyte activation and promotes transfer of astrocytic mitochondria to neurons against ischemic stroke. Redox Biol 54:102363. https://doi.org/10.1016/j.redox.2022.102363

Orr AG, Orr AL, Li X-J, et al (2009) Adenosine A2A receptor mediates microglial process retraction. Nat Neurosci 12:872–878. https://doi.org/10.1038/nn.2341

Peart JN, Gross GJ (2006) Cardioprotective effects of acute and chronic opioid treatment are mediated via different signaling pathways. Am J Physiol Heart Circ Physiol 291:H1746-53. https://doi.org/10.1152/ajpheart.00233.2006

Pu X, Liu J, Wang Y, et al (2025) Ginsenoside Rb1 attenuates coronary microvascular inflammatory injury via NDUFS4-SIRT5-DUSP1-mediated mitochondrial quality control in a murine ischemia-reperfusion model. J Ginseng Res 49:509–522. https://doi.org/10.1016/j.jgr.2025.04.006

Rebola N, Simões AP, Canas PM, et al (2011) Adenosine A_{2A} receptors control neuroinflammation and consequent hippocampal neuronal dysfunction. J Neurochem 117:100–111. https://doi.org/10.1111/j.1471-4159.2011.07178.x

Shaukat A, Shaukat I, Rajput SA, et al (2021) Ginsenoside Rb1 Mitigates Escherichia coli Lipopolysaccharide-Induced Endometritis through TLR4-Mediated NF-κB Pathway. Molecules 26:7089. https://doi.org/10.3390/molecules26237089

Skopál A, Kéki T, Tóth PÁ, et al (2022) Cathepsin D interacts with adenosine A2A receptors in mouse macrophages to modulate cell surface localization and inflammatory signaling. J Biol Chem 298:101888. https://doi.org/10.1016/j.jbc.2022.101888

Smith JA, Das A, Ray SK, Banik NL (2012) Role of pro-inflammatory cytokines released from microglia in neurodegenerative diseases. Brain Res Bull 87:10–20. https://doi.org/10.1016/j.brainresbull.2011.10.004

Taskén K, Aandahl EM (2004) Localized Effects of cAMP Mediated by Distinct Routes of Protein Kinase A. Physiol Rev 84:137–167. https://doi.org/10.1152/physrev.00021.2003

Teresa Bengoechea-Alonso M, Pelacho B, Osés-Prieto JA, et al (2003) Regulation of NF-κB activation by protein phosphatase 2B and NO, via protein kinase A activity, in human monocytes. Nitric Oxide 8:65–74. https://doi.org/10.1016/S1089-8603(02)00143-X

Tozzi A, Tscherter A, Belcastro V, et al (2007) Interaction of A2A adenosine and D2

dopamine receptors modulates corticostriatal glutamatergic transmission. Neuropharmacology 53:783–789. https://doi.org/10.1016/j.neuropharm.2007.08.006

Wang P, Lin C, Wu S, et al (2018) Inhibition of Autophagy is Involved in the Protective Effects of Ginsenoside Rb1 on Spinal Cord Injury. Cell Mol Neurobiol 38:679–690. https://doi.org/10.1007/s10571-017-0527-8

Wang X, Liu Y, Li J, et al (2024) GPCR-Gs mediates the protective effects of ginsenoside Rb1 against oxygen-glucose deprivation/re-oxygenation-induced astrocyte injury. J Tradit Chin Med Sci 11:33–43. https://doi.org/10.1016/j.jtcms.2023.11.002

Wang Y, Mou C, Hu Y, et al (2025) In vivo metabolism, pharmacokinetics, and pharmacological activities of ginsenosides from ginseng. J Ginseng Res 49:479–487. https://doi.org/10.1016/j.jgr.2025.05.003

Zhang H, Chen X, Wang X, et al (2021) Ginsenoside Rb1 attenuates lipopolysaccharide-induced neural damage in the brain of mice via regulating the dysfunction of microglia and astrocytes. J Integr Neurosci 20:813. https://doi.org/10.31083/j.jin2004084

Zhuang S, Shi F, Cannella N, et al (2025) Pharmacological Mechanism and Drug Research Prospects of Ginsenoside Rb1 as an Antidepressant. Antioxidants 14:238. https://doi.org/10.3390/antiox14020238